Quenching Heat Transfer Characteristics of Copper Rod in Saturated and Various Subcooled Condition

H. Zeol, M. Z. Sulaiman, H. Z. Hui, H. Ismail, and T. Okawa

Abstract This study investigated the quenching performance of a copper rod with 50 mm length and diameter of 20 mm. The specimen was heated to 600 °C as the initial temperature and immersed in a quenching pool of pure water (distilled water) followed with a subsequent quench seven times. Under atmospheric pressure, the experiments are conducted in saturated and various subcooled conditions (90, 80 and 60 °C). The cooling curves (temperature vs time) and the cooling rate curves (°C/s) of the copper cylinder are obtained from the experiment. Results show that the cooling performance for 1st quench and the subsequent quench for saturated and 90 °C subcooled condition shows a different performance related to the formation of the oxide layer at the copper surface that changes the surface characteristic. Vice versa, the cooling performance in 80 °C and 60 °C subcooled conditions has consistent performance for all quench, which is believed to be the domination of the subcooling effect, even though the physical surface appearance shows the same. Overall, the cooling curve of the copper rod was enhanced with the increase of subcooled temperature, especially for 60 °C subcooled conditions. The cooling curves for the subcooled of 90 and 80 °C still maintain the slope with the three-section shape, which is similar for the saturated case, but for the 60 °C subcooled conditions, the cooling curve slope suddenly increased and shifted to the left, showing the drastic decrease of centre temperature and the impact on the highly subcooled condition. The cooling rate curve shows the increasing peak value of cooling rate with increasing the subcooled temperature, which is the highest value during quench in 60 °C conditions. The minimum heat flux (MHF) point temperature rises and occurs faster, and the Critical Heat Flux (CHF) point is achieved early with the increasing subcooled temperature. The highly subcooled condition 60 °C shows no film boiling regime formation and the MHF point location is not visible.

H. Zeol · M. Z. Sulaiman (✉) · H. Z. Hui · H. Ismail
Faculty of Mechanical and Automotive Engineering Technology, Universiti Malaysia, 26600 Pekan, Pahang, Malaysia
e-mail: zuhairi@ump.edu.my

T. Okawa
Department of Mechanical and Intelligent Systems, The University of Electro-Communications, 1-5-1, Chofugaoka, Chofu-shi, Tokyo 182-8585, Japan

M. Y. Ismail et al. (eds.), *Technological Advancement in Mechanical and Automotive Engineering*, Lecture Notes in Mechanical Engineering,
https://doi.org/10.1007/978-981-19-1457-7_29

Keywords Quenching heat transfer · Minimum heat flux · Subcooling

1 Introduction

Quenching heat transfer is a rapid cooling process of a hot object that immerse in a colder fluid bath. Quenching is a widely used process for achieving martensitic and bainitic structures where its related to the heating and subsequent rapid cooling rate procedure to increase the hardness of metal [1]. Quenching is vital as a safety procedure in heavy industry, especially in the nuclear industry, acting as an emergency core cooling system (ECCS) in a nuclear reactor. It plays a significant role as a countermeasure during the loss of coolant accident (LOCA) in nuclear reactors [2]. During quenching, heat transfer rates are restricted when the film boiling occurs, where a stable vapour layer covers the hot object's surface. This occurrence creates a strong resistance to energy transfer between the two surfaces [3]. Cooling curve and cooling rate curve analysis is commonly used to observe the quenching performance of the test object since it is the most comprehensive way to characterise a quench media. The cooling curve is produced when a material that is initially at a temperature above the boiling of the quench media is introduced into the quench media [4]. Leidenfrost point or known as minimum film boiling (MHF) was focused by researchers to determine the performance of the cooling rate during the quenching process, which is with the early time to achieve MHF point, will contribute to the early ends of film boiling regime, then accelerate the cooling rate [5]. Many factors are related with the formation of the stable film boiling regime, and one of the main factor is the liquid temperature, either in saturated or in subcooled condition [6].

Many researchers investigate the effect of the subcooled condition on quenching performance. In 2007, Bolukbasi et al. [7] studied vertical brass cylinder quenching performance with five different dimensions in saturated and various subcooled conditions. The specimen was heated up until 600 °C, then directly quenched in a quenching pool. The result shows that in the saturated condition, three sections shape the graph, representing the film boiling regime, nucleate boiling regime, and natural convection cooling regime. However, the film boiling regime was not occurring at subcooled conditions for all specimens because the film or the vapour blanket was demolished at higher temperatures. They believe the heat transfer occurred at nucleate boiling and the natural convection stage.

Similar to Lotfi et al. [8], they experimented with examining the quenching performance of a silver sphere in distilled water, Ag and TiO_2 water nanofluids with slightly a subcooled condition (90 °C). The result obtained shows that the film boiling started immediately after being immersed in the fluids. They noticed the formation of a thick and smooth vapour blanket covering the sphere during the film boiling regime. Then with decreasing the temperature, the vapour blanket collapse and solid-fluid start to contact each other. This shows the slightly subcooled condition will have a slight impact on the cooling process. In 2017, Young et al. [9] experimented with tabilize the effect of subcooling on quenching performance. They use a zircaloy rod specimen

with an initial temperature of 600 °C, then quickly quench into the highly subcooled pure water (25 °C). They found that once the specimen dropped into the quench pool, the temperature centre decreased drastically. They discovered that the liquid subcooling had a significant influence on the quenching curve and phenomena. The liquid subcooling increased led to shifting the quenching curve to the left (decreasing the quenching duration).

Lee et al. [10] investigated the quenching performance of the zircaloy-4 and Cr-alloy-coated cladding tubes in saturated and 50 °C subcooled pure water. Both specimens were heated up to 600 °C and then subsequent quenched into the quench pool three times. They discovered that the cooling curve for both specimens shows the decreasing of surface temperature exponentially in the nucleate boiling regime. Using a high-speed camera, both specimens show vapour film formation in the early stage during quench in saturated fluid, but no vapour film boiling was observed during quench in a subcooled fluid. In 2021, Wang et al. [11] investigate the quenching performance of the FeCrAl rodlets in various subcooled (95, 90, 85 and 80 °C) in distilled water. The specimen was prepared with two types: bare and rough surfaces with 0.2 μm and 1.6 μm, respectively. Both have an initial temperature of 600 °C. They found that the cooling rate performance for both specimens shows increment trending, in which the cooling curve slope becomes steeper and shifts to the left with increasing the liquid subcooling degree. Moreover, the quenching time is shorted, and the MHF increases as the liquid subcooling degree increases.

Kang et al. [12] conducted an experiment to analyse the quenching performance of 2 types of surface of zirconium vertical rod specimen, which are completely wettable surface (CWS) and Bare surface (BZS) with an initial temperature of 800 °C in saturated and various subcooled distilled water. They found that the cooling curve is strongly related to surface hydrophilicity and the subcooling fluids condition. Both specimens show great enhancement of cooling rate with shorted time as the subcooling degrees increase. Direct quenching without stable film boiling regime shows at 60 K subcooled for CWS, and >15 K subcooled for BZS specimen, which indicates the early collapse of vapour film blanket.

Similar to Ebrahim et al. [13], they researched quenching performance in saturated and subcooled liquid using three different cylinder shape specimens: stainless steel (S.S.), Zirconium (Zr), and Inconel-600 rods with an initial temperature of 550 °C. For all types of specimens, they identified that subcooling strongly influences the temperature of the MHF point. As the liquid subcooling increases, the heat transfer increases due to the higher driving temperature difference between the heated surface and the ambient liquid temperature.

In addition, in 2020, Xiong et al. [14] conducted an experiment of quenching performance of two types of the specimen which are FeCrAl alloy and Zircaloy-4 with initial temperature 600 °C in both saturated and various subcooled conditions (80, 85, 90 and 95 °C) of distilled water. They noticed a similar result, which is the cooling curves shifted to the left for both specimens. Using a high-speed camera, they observed that the liquid-vapour interface's evaporation is weak and the vapour film is thin in the large subcooling cases, which confirmed that more portion of heat flux is tabiliz to heat up the subcooled liquid in the film boiling regime.

However, the temperature of the specimen can also significantly influence the formation of a stable film boiling regime, although the surrounding fluids were in highly subcooled condition. In 2015, Hsu et al. [15] experimented with investigating the quenching performance of stainless steel and zircaloy spheres in both de-ionised and natural seawater at 33 °C subcooled conditions. The initial temperature for both specimens was set up for a very high temperature which is 1000 °C. The cooling curves obtained for quenching in de-ionised water show the formation of the stable film boiling regime, which lasts about 16 s for stainless steel and 12 s for zircaloy specimen. Further investigation with a high-speed camera tabilizeson found the small bubble nucleated at the surface. Then the stable vapour blanket is formed, although initially the interface is initially unstable due to the transient contact at the sphere surface, but tabilizes within a short period.

Based on the aforementioned literature, it is found that most of the research in quenching performance in distilled water, seawater and recent nanofluids either in saturated and various subcooled conditions. On top of that, most of the experiments used quenching metal with surface coated treatment or alloy types such as stainless steel, zircaloy, FeCrAl, brass, copper coated with nickel or other metal alloy and coated surface metal as the specimen due to the low thermal conductivity characteristics and to avoid any surface degradation due to the oxidation layer occurred when the metal exposed at the very high temperature during the quenching process [16].

This paper aims to evaluate the quenching heat transfer performance based on a cooling curve using subsequent quenches of untreated surface copper rod metal (without any surface coating) in saturated and subcooled distilled water and qualitative evaluation of the physical surface changes during the subsequent quenched of this copper rod specimen.

2 Methodology

2.1 Experimental Setup

Figure 1 shows the schematic drawing for the copper cylinder rod specimen (50 mm × 20 mm diameter), while Fig. 2 shows the picture for details apparatus setup for the quenching experiment. This experiment involved several main components; 20 L closed stainless steel bath tanks combined with JULABO circulator, S.Y. Electric melting furnace, and a NiDAQ data acquisition system. Ungrounded K-type thermocouples MISUMI with a 1 mm diameter were used and inserted at the centre of the copper rod to record the centre temperature measurement during the experiment. The uncertainty for temperature measurement is ±1.5 °C. National Instruments data acquisition (NiDAQ) was used to measure temperature time during the quenching process. The automatic quenching system was designed by installing the AitTAC pneumatic air cylinder with a compressed air supply to get the same speed of specimen movement during the quenching process for all quenching experiments. 80 mm

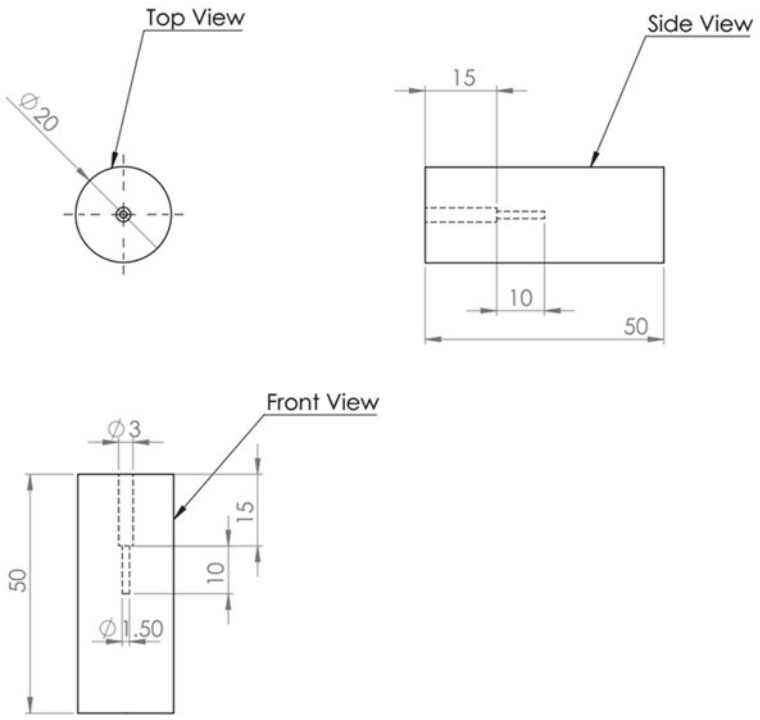

Fig. 1 Details schematic drawing for copper rod specimen

borosilicate was prepared as a quenching pool (180 × 130 mm diameter). The furnace and copper rod were placed directly above the quench pool at the prepared platform on top of the quench pool. The copper rod was placed into the furnace while attached to a pneumatic cylinder. Table 1 shows the details about the apparatus used during the quenching experiment.

2.2 Experimental Procedure

The experiment was started with heat up the distilled water in a closed stainless steel tank until it achieved 60 °C, then maintained that temperature. 1500 ml distilled water was prepared in a beaker then placed into a closed stainless steel tank, then waited until it achieved an equilibrium temperature (60 °C) with surrounding distilled water in the tank. Simultaneously, the copper rod was prepared to get a mirror surface. The copper rod's surface was prepared using different sizes of the grit of sandpaper, which are 800, 1000, 2000, 5000 and 7000, then final polishing by using polish metal paste. Lastly, the copper rod was cleaned using acetone and distilled water. After finishing preparing the copper rod surface, the copper rod was fixed at the quench rod and

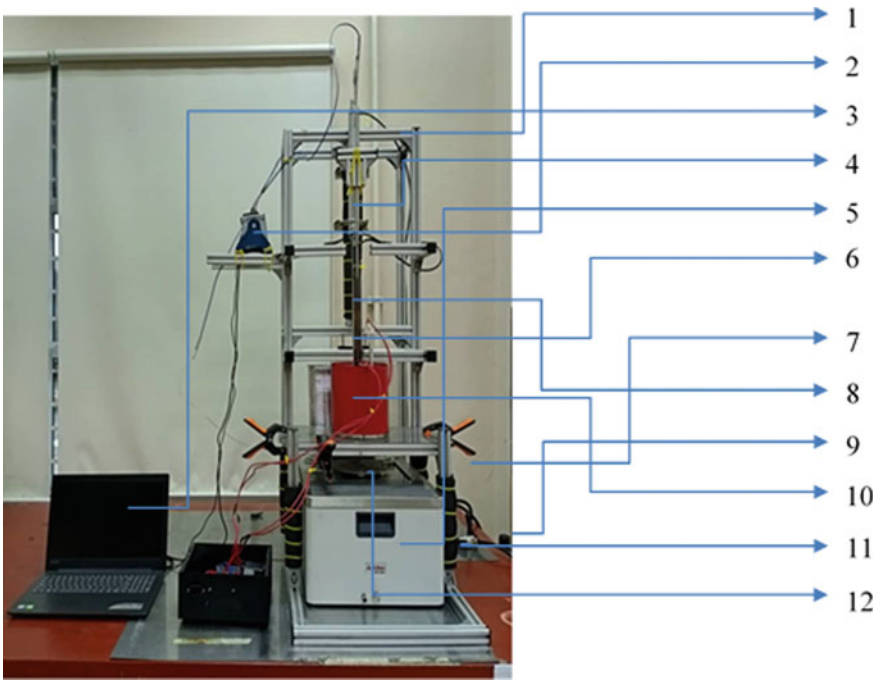

Fig. 2 Quenching heat transfer apparatus setup

inserted into the furnace to heat up until it achieved 600 °C initial temperature. Once the desired temperature was reached, the furnace was turned off and quickly immersed into the quench pool using an air valve controller. The experiment was ended once the thermal equilibrium was achieved between the copper rod and the distilled water in the quench pool. The rod was subsequently quenched repetitively seven times afterwards with the same copper surface without washing the surface during the repetition tests to investigate the surface effect on the rate of heat transfer. The temperature-time data from the quenching process were collected and analysed. After finishing all the procedures, the experiment was repeated by changing the temperature of the quench pool to 80, 90 and 100 °C.

3 Result and Discussion

Figure 3a shows the cooling curves with multiple quenches of copper rod in distilled water at saturated condition, while Fig. 3b shows the cooling rate curves. Both cooling curves and cooling rate curves are divided into three-section shapes, representing the cooling process that involved three main regimes: film boiling regime, nucleate boiling regime, and natural convection cooling regime [17]. These curves also consist

Table 1 Apparatus used during quenching

No	Name	Description
1	Quenching Rig	– Aluminum profile as the main structure for quenching rig
2	NiDAQ Data Logger	– Collecting the temperature data from thermocouple
3	Laptop	– To receive temperature data from the data logger
4	Pneumatic Piston Cylinder	– AirTAC brand – 300 mm stroke with 10 bar maximum pressure
5	JULABO Tank with Circulator	– JULABO brand – Maintain the desired subcooled temperature
6	Quenching Rod	– 8 mm O.D. diameter Stainless Steel 316L pipe – Attached with the specimen and fitted with cylinder piston
7	Fitting coupling	– Joint supply from air compressor supply sources
8	Thermocouple	– MISUMI brand grounded type – Type-K thermocouple with 1 mm probe diameter
9	Air Regulator	– AirTac brand. Control and filter air pressure input – 10 bar of maximum pressure
10	Electrical Furnace	– S.Y. Electric Melting Furnace – 1100 °C maximum running temperature
11	Hand valve pneumatic controller	– AirTac brand – 3 step position control valve, 8 bar maximum pressure
12	Beaker (Pool Quench)	– 2000 ml beaker volume as quench pool

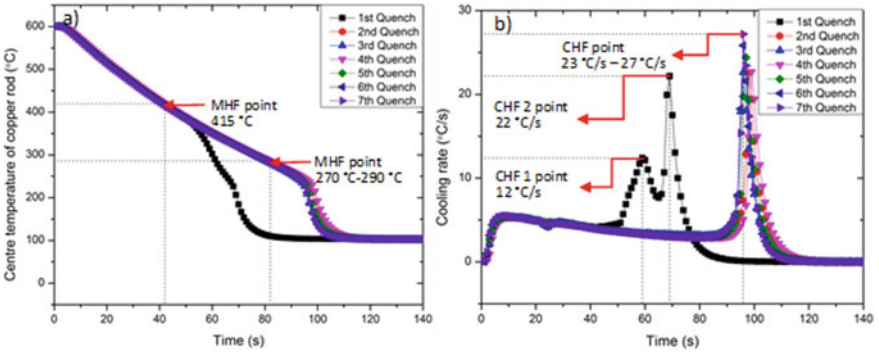

Fig. 3 The quenching performance of copper rod in distilled water at saturated condition; **a** Cooling curve, and **b** Cooling rate curve

of two main reference points known as minimum heat flux (MHF), which represent the transition point from film boiling to nucleate boiling [8], and critical heat flux (CHF) at where the point of the maximum boiling heat transfer [18]. The formation of film boiling regime acting as a resistant layer between the surface and water decreased the heat transfer from the surface to the water, decreasing the cooling rate [7].

It can be seen in Fig. 3a, the 1st quench cooling curve for clean surface shows the fastest cooling time, where the minimum heat flux point (MHF) is located at a temperature which is 415 °C and occur at the quickest time, which is after 43 s of quenching. After that, the subsequent quench using the same unwashed copper rod shows the decreasing of cooling time with a longer time taken for the rod to cool. It can be observed that the cooling curve data scattered almost the same for the 2nd quench until the 7th quench, which is the MHF point temperature is between 270 and 290 °C and the time taken for the MHF to occur is between 80 and 84 s.

As shown in Fig. 3b, it could be clearly seen that double CHF point (double peak of cooling rate) could be observed during the 1st quench. A similar observation was observed in the study of Umehara et al. [19] in quenching of the stainless steel in nanofluids, but the next subsequent quench had only a single CHF point noticed. The CHF 1 point during 1st quench happened at 59 s after the quench and had a peak cooling rate value of about 12 °C/s. The CHF 2 point happened at 69 s, and the peak value of cooling rate recorded about 22 °C/s, which almost had the same reading as the subsequent quench after that (23–27 °C/s). However, the CHF point for the subsequent quench happened at about 98, 38 s later than CHF 1 and 28 s later than CHF 2.

The different performance for the first quench (shown in Figs. 3a and b) and with subsequent quench is suspected to the formation of the oxidation layer at the copper rod surface (as shown in Fig. 4c–h). It should be noted that the copper surface with high thermal conductivity of 386 W/m K at 20 °C [20] was susceptive to thin oxide layer formation at the surface, and qualitative observation was shown in Fig. 4b. Following the first quench with polished surface, oxidation started to appear. After a series of subsequent quench, the copper rod surface is now fully coated with the oxidation layer, as depicted in Fig. 4c–h. It is believed the oxidation affect the copper surface' thermal conductivity characteristic and subsequently becomes the insulation barrier that leads to the degradation of the heat transfer from the copper surface to the surrounding fluids, hence prolonging the time needed to cool the rod as previously discussed by Sher et al. [16].

Figure 5a shows the cooling curves, while Fig. 5b shows cooling rate curves with multiple quenches of copper rod in distilled water at 90 °C, which is in slightly subcooled condition. The cooling curve in Fig. 5a maintained the three-section shape graph. The 1st quench with a clean and polished surface shows the fastest cooling time, where the MHF point was located at a higher temperature, at 463 °C, which is an increment of 10% compared to the MHF of the 1st quench in a saturated condition (see Fig. 3a). Respective to the cooling time enhancement, the time taken to achieve MHF point is about 22 s, a 49% reduction of time taken compared in a saturated condition. As depicted in Fig. 5a, the subsequent quench using the same unwashed

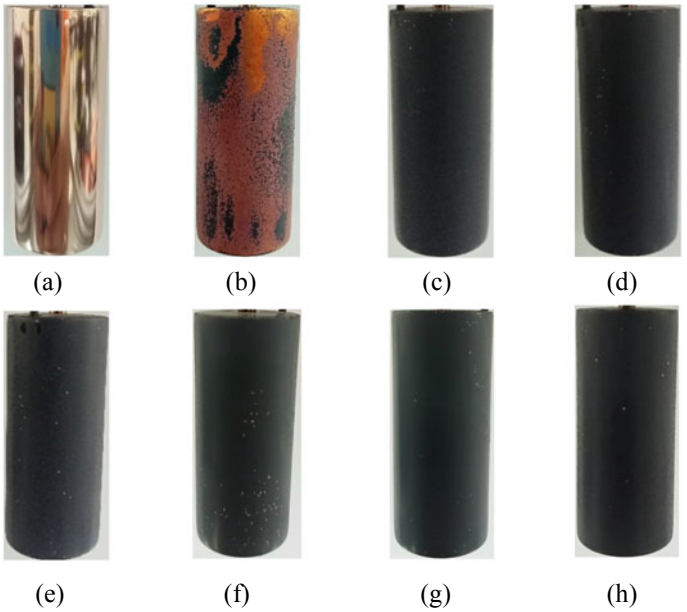

Fig. 4 The surface structure of copper rod during quenching in distilled water at saturated condition **a** after polishing, **b** 1st quench, **c** 2nd quench, **d** 3rd quench, **e** 4th quench, **f** 5th quench, **g** 6th quench and **h** 7th quench

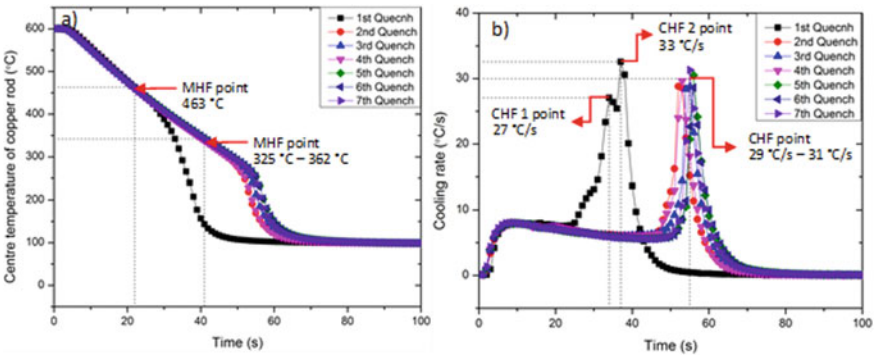

Fig. 5 The quenching performance of copper rod in distilled water at 90 °C subcooled conditions; **a** Cooling curve, and **b** Cooling rate curve

copper rod shows the decreasing of cooling time with a longer time taken to cool the rod. The subsequent quenching from the 2nd quench until the 7th quench also shows minimal changes in the graph pattern. The MHF point temperature for these series of quenching processes is between 325 °C and 362 °C, which between 17 and 20% of increment and the time taken to achieve this MHF point is between 37 and 44 s,

reduction of time about 48%–54% compared to the case in a saturated condition, respectively (see Fig. 3a).

As shown in Fig. 5b, two peaks for the CHF point, which is similar to the case in saturated condition could also be seen. However, CHF 1 is nearly unnoticeable. The CHF 1 point during 1st quench happened at 34 s (42% reduction of time compared to saturated condition), just slightly early about 3 s compared to CHF 2 point, which occurred at 37 s (46% reduction of time compared to saturated condition) after the quench. The peak cooling rate value for CHF 1 recorded about 27 °C/s (54% increment compared to saturated condition), slightly lower than CHF 2 point, which is about 33 °C/s (29% increment compared to saturated condition). Afterwards, the subsequent quench from the second to the seventh showed almost the same peak cooling rate value between 29 and 31 °C/s. These denoted the enhancement of 13–21% of cooling rate compared to those in a saturated condition. The time duration to achieve this point was about 55 s, and this is a 44% reduction of time compared to saturated conditions.

As shown in Fig. 6c–h, the fully coated oxidation layer at the copper rod surface could be seen, and this is also obtained in case of saturated condition (see Fig. 4c–h). The different quenching performance for 1st quench with subsequent quench is due to the oxidation layer discussed in saturated condition quenching performance. Based on the cooling curves and cooling rate curve obtained, the cooling process occurs

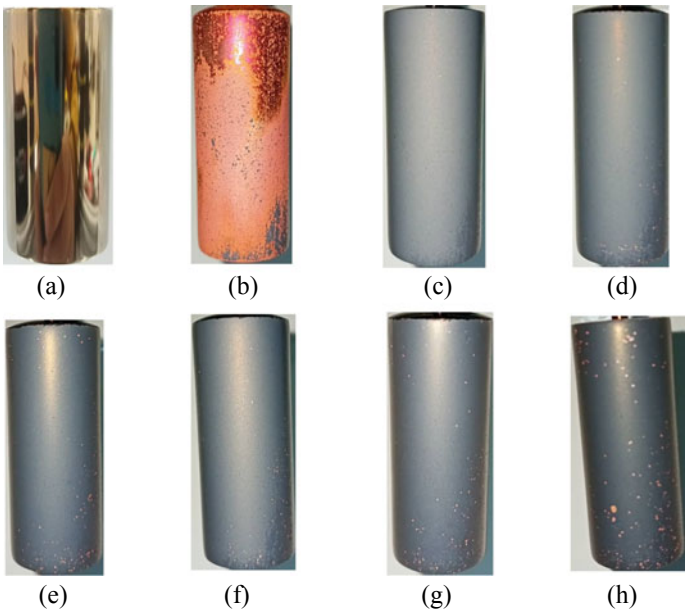

Fig. 6 The surface structure of copper rod during quenching in distilled water at slightly subcooled condition 90 °C **a** after polishing, **b** 1st quench, **c** 2nd quench, **d** 3rd quench, **e** 4th quench, **f** 5th quench, **g** 6th quench and **h** 7th quench

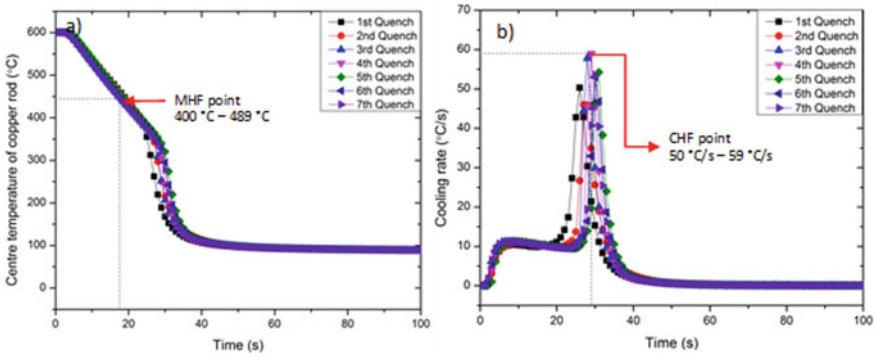

Fig. 7 The quenching performance of copper rod in distilled water at 80 °C subcooled conditions; **a** Cooling curve, and **b** Cooling rate curve

slightly faster than in saturated conditions. It clearly shows the effect of slightly subcooled conditions towards the quenching performance, which is similar to the results obtained by Lotfi et al. [8].

Figure 7a and b shows the cooling curves and cooling rate curves with multiple quenches of copper rod in distilled water at 80 °C subcooled conditions. Figure 7a Cooling curves maintained the three-section shape graph but with a high slope value, representing the high cooling rate. As referred to the curves, there is not much distinct cooling performance between the 1st quench and subsequent quench. In Fig. 7a, the MHF point was recorded at the temperature between 400 and 489 °C, which is an increment of between 5 and 10% compared to quench in 90 °C subcooled conditions (see Fig. 5a). The time taken to achieve MHF point is about 15–18 s, which is a 32–59% reduction of time compared to 90 °C subcooled conditions. The 1st quench performance has not much different from the subsequent quench that is in contrast with the result in saturated (see Fig. 3a) and 90 °C subcooled conditions (see Fig. 5a).

As shown in Fig. 7b, there is no formation of the double peak cooling rate value (double CHF point) during the 1st quench, which in contrast to the result obtained in saturated (see Fig. 3b) and 90 °C subcooled conditions (see Fig. 5b). The peak value of cooling rate for all quenching nearly similar performance ranging between 50 and 59 °C/s. It shows a significant increment of about 44–46% compared to 90 °C subcooled conditions. The quenching time taken to achieve the CHF point ranges between 26 and 31 s after the quench, which is a 24–44% reduction of time compared to 90 °C subcooled conditions (see Fig. 5b).

As shown in Fig. 8, the oxidation layer also occurred with the same pattern as shown in Fig. 8c–h. However, the cooling performance shows a different pattern with saturated (see Fig. 3a and b) and 90 °C subcooled conditions (see Fig. 5a and b). These phenomena are due to the domination of the subcooled condition factor towards the quenching performance. In 80 °C subcooled conditions with higher subcooling conditions, more heat is needed for sensible heat of the fluids surrounding, thinning the vapour film of vapour blanket during the film boiling regime [21]. Since in the

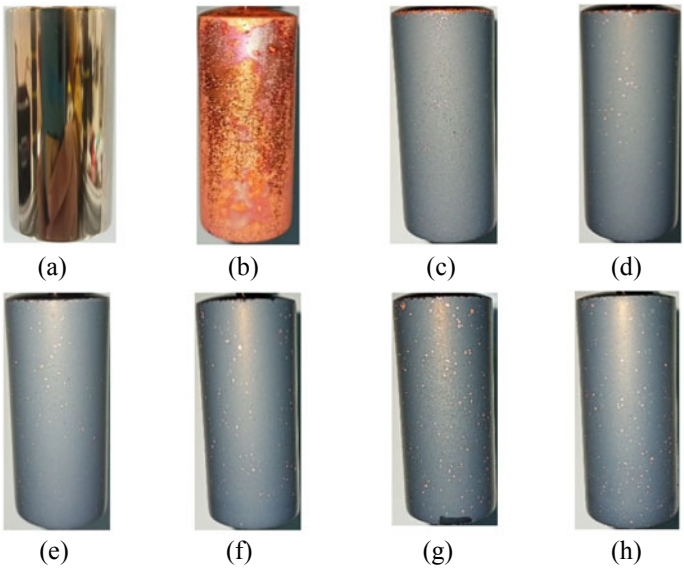

Fig. 8 The surface structure of copper rod during quenching in distilled water at subcooled condition 80 °C **a** after polishing, **b** 1st quench, **c** 2nd quench, **d** 3rd quench, **e** 4th quench, **f** 5th quench, **g** 6th quench and **h** 7th quench

present case, the 600 °C initial temperature of the specimen was insufficient to supply heat to sustain the formation of stable film boiling for a longer time. It is proven in previous research conducted by Nishio et al. [18] that the MFH temperature is proportional to the liquid subcooling, which is the higher liquid subcooling requires a higher temperature of the test specimen. Under a higher liquid subcooling condition, more heat is needed to sufficiently heat the surrounding fluid to form a stable vapour film.

Figure 9a and b shows the cooling curves and cooling rate curves with multiple quenches of copper rod in distilled water at 60 °C, which is in highly subcooled condition. The cooling curve in Fig. 9a depicted a steeper negative slope value representing the high cooling rate. From the cooling curves recorded, there is no clear visible three-section shape as obtained in the saturated (see Fig. 3a), 90 °C subcooled conditions (see Fig. 5a), and 80 °C subcooled conditions (see Fig. 7a). Once the specimen dropped into the highly subcooled water pool, the centre temperature decreased suddenly. Then, the boiling regime was changed quickly to the single-phase natural convection regime. In other words, the stable film boiling regime did not seem to be observed clearly for the present highly subcooled water condition, which is no stable vapour blanket happened. The vapour blanket is suspected of collapsing directly once the copper rod specimen quench in the distilled water, leading to the liquid-solid directly contacting each other [14]. The time taken for the copper rod specimen to cool down from the initial temperature of 600 °C to the saturation point of water of 100 °C takes about 22 s. With the large value of liquid subcooling, more portions

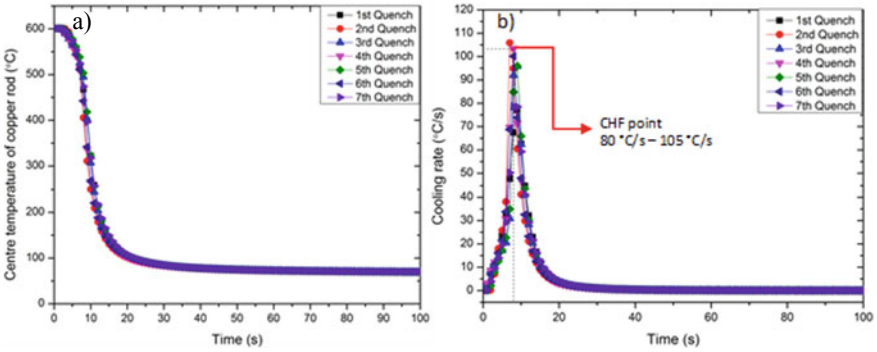

Fig. 9 The quenching performance of copper rod in distilled water at 60 °C subcooled conditions; **a** Cooling curve, and **b** Cooling rate curve

of the heat flux are used to heat the liquid surrounding, then the evaporation on the liquid-vapour interface is weak, and the vapour film is thin [14].

As depicted in Fig. 9b, the peak cooling rate was recorded at a very high value between 80 and 105 °C/s and its occurred less than 10 s, which is an extremely high cooling rate. As refer to Figs. 3b, 5b, 7b and 9b, the peak value of cooling rate trending shows increasing and the time to achieve CHF point shortened with increase the subcooled temperature. The increment was expected due to the rise in the subcooled temperature. The vapour film collapses early at high temperature, then re-establish the liquid-solid contact with rapid boiling with a sharp rise peak of cooling rate value at the copper rod surface [22].

Although the oxidation layer appearance as shown in Fig. 10 of the copper surface still have the same with others condition, the factor of the highly subcooled condition becomes dominant factors, then contribute to the curves obtained. The same issues were discussed for the quenching performance in 80 °C subcooled conditions, hence confirmed again with the result obtained by Nishio et al. [18].

Figure 11a shows the compilation of 1st cooling curves performance, while Fig. 11b shows the compilation of 1st cooling rate curves of copper rod in distilled water for all conditions, which is in saturated, 90 °C, 80 °C, and 60 °C subcooled conditions. As could be referred to in the cooling curves in Fig. 11a, the quenching performance sequential shift to the left as the fluids temperature decreases. The cooling curves for the subcooled of 90 and 80 °C still maintain the three-section shape similar to the saturated case. Quenching performance in saturated conditions shows the longer time taken to cool the rod. The MHF point temperature was recorded at 415 °C and occurred at 43 s after quenching. When the liquid is slightly subcooling 10 °C (90 °C subcooled conditions), the quenching time is markedly shortened to about 22 s at the temperature of 463 °C, equivalent to a relative acceleration by a factor of 49% to the saturated case. At the highest subcooling degree tested (60 °C subcooled conditions), the quenching time is below 20 s, corresponding to a relative cooling time enhancement by over 75% compared to saturated conditions.

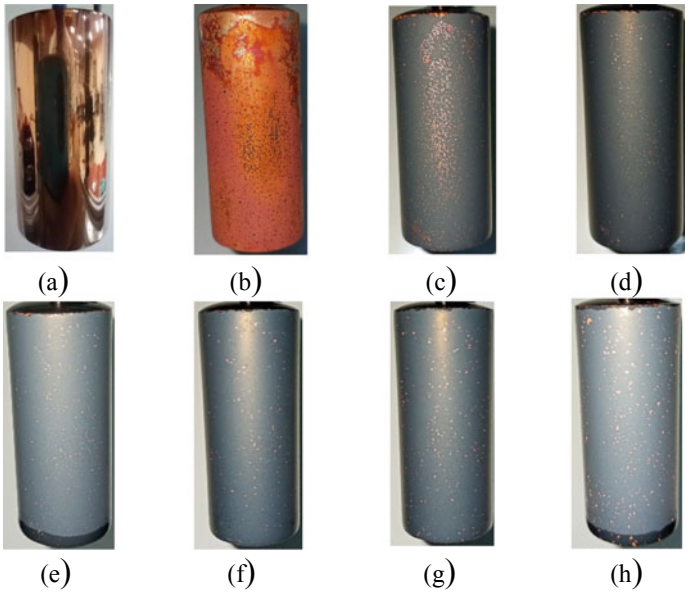

Fig. 10 The surface structure of copper rod during quenching in distilled water at highly subcooled condition 60 °C **a** after polishing, **b** 1st quench, **c** 2nd quench, **d** 3rd quench, **e** 4th quench, **f** 5th quench, **g** 6th quench and **h** 7th quench

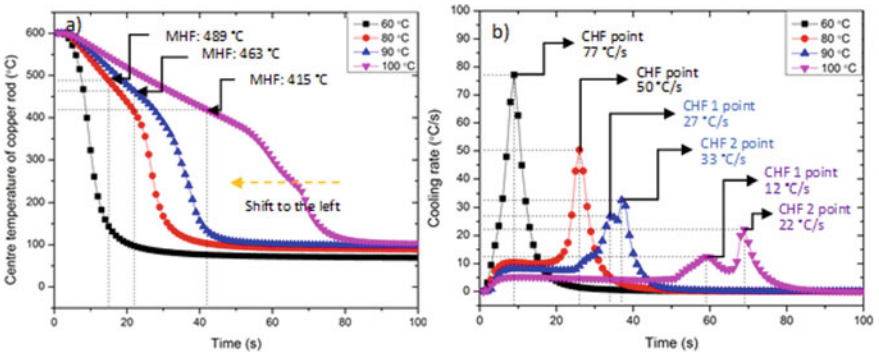

Fig. 11 The compilation of the 1st quench performance of copper rod in distilled water at saturated, 90, 80, and 60 °C subcooled conditions; **a** Cooling curve, and **b** Cooling rate curve

The cooling rate curve in Fig. 11b shows the same trend, which is with increasing the subcooled temperature, the value of the peak cooling rate becomes higher and the time taken to achieve the CHF point shortened. The highest value of the peak cooling rate is recorded about 77 °C/s during 1st quench in 60 °C subcooled condition, which is the increment of about 71% compared to CHF 2 in saturated condition and the time taken to achieve the CHF point during 1st quench in 60 °C subcooled conditions is

about 9 s, which is 85% reduction of time compared to CHF 2 in a saturated condition. The double CHF (double peak cooling rate) was only visible during the 1st quench in saturated and 90 °C subcooled conditions, while for the subcooled 80 and 60 °C conditions, the double CHF was invisible. The quenching heat transfer enhancement upon increasing the subcooling degree is significantly attributed to the increasing temperature difference between the copper rod and liquid pool. Similar result with Fan et al. [23], they discovered that the cooling curves obtained were shifted to the left with sequentially increasing the slope value. They agreed that this enhancement is due to the temperature difference between the specimen and surrounding fluid.

4 Conclusion

In this study, the quenching heat transfer characteristics in different quenched conditions have been explored by performing the quenching experiments of a heated copper rod in distilled water at saturated and various subcooled conditions (60, 80, and 90 °C). A rod with 20 mm in diameter and 50 mm in length at the initial temperature of 600 °C was tested. The following results were obtained:

(a) The quenching performance in saturated shows the longer time taken to cool the rod. The three-section shape is clearly shown with the formation stable film boiling regime. There are two CHF points noticed in the cooling rate curve during 1st quench in saturated.
(b) In the slight subcooled condition of fluids (90 °C), the performance of the cooling rate has shown an enhancement with an increment of the peak cooling rate value and shortened the time to achieve CHF point, and double CHF point observed in the first quench.
(c) Both cooling performances of saturated and 90 °C subcooled conditions show a gap of cooling rate between the 1st quench and the subsequent quench, which is believed due to the formation of the oxidation layer at the copper rod surface.
(d) Cooling curve slopes in 80 °C subcooled conditions increase significantly, incrementing the peak cooling rate value and reducing the time to achieve CHF compared to saturated and 90 °C subcooled cases. Cooling curves data in 80 °C subcooled shows almost the same for all quench, although the same surface structure is obtained, which is due to the domination of the subcooled factors towards the quenching performance, with the low initial temperature of the specimen (600 °C).
(e) The cooling curve for the highly subcooled condition (60 °C) did not maintain the three-section shape, which the MHF point did not seem to be observed. The centre temperature decreases suddenly during quenching. The peak cooling rate and the time taken to achieve CHF point recorded the highest and faster value compared to others subcooled and saturated.

Acknowledgements Financial support by the Malaysian Ministry of Height Education under FRGS (FRGS/1/2019/TK07/UMP/02/2) and Universiti Malaysia Pahang (www.ump.edu.my) under PGRS2003148 are gratefully acknowledged. We wish to express our gratitude to all the staff in Universiti Malaysia Pahang that involved in the experimental work. Last but not least, thank you to the first author's wife, Nur Fatehah Binti Md Shakur for the continuous moral support and motivation during his study journey.

References

1. Babu K, Prasanna Kumar TS (2011) Effect of CNT concentration and agitation on surface heat flux during quenching in CNT nanofluids. Int J Heat Mass Transf 54(1–3):106–117. https://doi.org/10.1016/j.ijheatmasstransfer.2010.10.003
2. Fu BR, Ho YH, Ho MX, Pan C (2016) Quenching characteristics of a continuously-heated rod in natural seawater. Int J Heat Mass Transf 95:206–213. https://doi.org/10.1016/j.ijheatmasstransfer.2015.11.093
3. Kim H, DeWitt G, McKrell T, Buongiorno J, wen Hu L (2009) On the quenching of steel and zircaloy spheres in water-based nanofluids with alumina, silica and diamond nanoparticles. Int J Multiph Flow 35(5): 427–438. https://doi.org/10.1016/j.ijmultiphaseflow.2009.02.004
4. Boyer HE, Archambault P, Moreaux F, Kobasko NI (1992) Techniques of quenching. In: Liscic B, Tensi HM, Luty W (eds) Theory and technology of quenching. Springer, Berlin, Heidelberg. https://doi.org/10.1007/978-3-662-01596-4_10
5. Lee GC, Kim SH, young Kang J, Kim MH, Jo HJ (2019) Leidenfrost temperature on porous wick surfaces: decoupling the effects of the capillary wicking and thermal properties. Int J Heat Mass Transf 145:118809. https://doi.org/10.1016/j.ijheatmasstransfer.2019.118809
6. Gylys J, Skvorcinskiene R, Paukstaitis L, Gylys M, Adomavicius A (2016) International journal of heat and mass transfer film boiling influence on the spherical body's cooling in sub-cooled water. Int J Heat Mass Transf 95:709–719. https://doi.org/10.1016/j.ijheatmasstransfer.2015.12.051
7. Bolukbasi A, Ciloglu D (2007) Investigation of heat transfer by means of pool film boiling on vertical cylinders in gravity. Heat Mass Transf und Stoffuebertragung 44(2):141–148. https://doi.org/10.1007/s00231-007-0238-7
8. Lotfi H, Shafii MB (2009) Boiling heat transfer on a high temperature silver sphere in nanofluid. Int J Therm Sci 48(12):2215–2220. https://doi.org/10.1016/j.ijthermalsci.2009.04.009
9. Young C, Kim S (2017) Parametric investigation on transient boiling heat transfer of metal rod cooled rapidly in water pool. Nucl Eng Des 313:118–128. https://doi.org/10.1016/j.nucengdes.2016.12.005
10. Lee KG, In WK, Kim HG (2019) Quenching experiment on Cr-alloy-coated cladding for accident-tolerant fuel in water pool under low and high subcooling conditions. Nucl Eng Des 347(November 2018):10–19. https://doi.org/10.1016/j.nucengdes.2019.03.017
11. Wang Z, Zhong M, Deng J, Liu Y, Huang H, Zhang Y (2021) Annals of nuclear energy experimental investigation on the transient film boiling heat transfer during quenching of FeCrAl. Ann Nucl Energy 150:107842. https://doi.org/10.1016/j.anucene.2020.107842
12. young Kang J, Lee GC, Kim MH, Moriyama K, Park HS (2018) Subcooled water quenching on a super-hydrophilic surface under atmospheric pressure. Int J Heat Mass Transf 117:538–547. https://doi.org/10.1016/j.ijheatmasstransfer.2017.09.006
13. Ebrahim SA, Chang S, Cheung FB, Bajorek SM (2018) Parametric investigation of film boiling heat transfer on the quenching of vertical rods in water pool. Appl Therm Eng 140(March):139–146. https://doi.org/10.1016/j.applthermaleng.2018.05.021
14. Xiong J,Wang Z,Xiong P, Lu T,Yang Y (2020) Experimental investigation on transient boiling heat transfer during quenching of fuel cladding surfaces. Int J Heat Mass Transf 148(xxxx):119131. https://doi.org/10.1016/j.ijheatmasstransfer.2019.119131

15. Hsu SH, Ho YH, Ho MX, Wang JC, Pan C (2015) On the formation of vapor film during quenching in de-ionised water and elimination of film boiling during quenching in natural sea water. Int J Heat Mass Transf 86:65–71. https://doi.org/10.1016/j.ijheatmasstransfer.2015.02.049
16. Sher I, Harari R, Reshef R, Sher E (2012) Film boiling collapse in solid spheres immersed in a sub-cooled liquid. Appl Therm Eng 36:219–226. https://doi.org/10.1016/j.applthermaleng.2011.11.018
17. Jan J, Company FM, Mackenzie DS (2020) On the development of parametrical water quenching heat transfer model using cooling curves by ASTM D6200 quenchometer on the characterisation of heat transfer rate in various boiling regimes using quenchometers and its application for quenching process. no. July 2020. https://doi.org/10.1007/s11665-020-04803-z
18. Nishio S, Uemura M, Sakaguchi K (1987) Film boiling heat transfer and Minimum-Heat-Flux (MHF)-point condition in subcooled pool boiling. JSME Int J 30(266):1274–1281. https://doi.org/10.1299/jsme1987.30.1274
19. Umehara Y, Okawa T, Enoki K (2019) Evaluation of the performance of nanofluid as quenching coolant. Tetsu-To-Hagane/J Iron Steel Inst Japan 105(11):1050–1058. https://doi.org/10.2355/tetsutohagane.TETSU-2019-035
20. Carvill J (1993) 3 - Thermodynamics and heat transfer. In: Carvill J (ed) Mechanical engineer's data handbook. Butterworth-Heinemann, pp 102–145. https://doi.org/10.1016/B978-0-08-051135-1.50008-X
21. Li JQ et al (2018) An experimental study of the accelerated quenching rate and enhanced pool boiling heat transfer on rodlets with a superhydrophilic surface in subcooled water. Exp Therm Fluid Sci 92(November 2017):103–112. https://doi.org/10.1016/j.expthermflusci.2017.11.023
22. Li JQ, Mou LW, Zhang YH, Yu JQ, Fan LW, Yu ZT (2018) Pool boiling heat transfer and quench front velocity during quenching of a rodlet in subcooled water: Effects of the degree of subcooling. Exp Heat Transf 31(2):148–160. https://doi.org/10.1080/08916152.2017.1397819
23. Fan L, Li J, Zhang L, Yu Z, Cen K (2016) Pool boiling heat transfer on a nanoscale roughness-enhanced superhydrophilic surface for accelerated quenching in water. Appl Therm Eng 109:630–639. https://doi.org/10.1016/j.applthermaleng.2016.08.131